TITLE

Identification of therapeutic targets of inflammatory monocyte recruitment to modulate the allogeneic injury to donor cornea.

AUTHORS

Thabo Lapp*[1,4], Sarah S. Zaher*[1,2], Carolin T Haas[1], David L Becker[3†], Chris Thrasivoulou[3], Benjamin M Chain[1], Daniel F P Larkin[§2], Mahdad Noursadeghi[§1]

AFFILIATIONS

[1]Division of Infection and Immunity, University College London, Gower St, London, UK

[2]NIHR Moorfields Biomedical Centre, Moorfields Eye Hospital, London, UK

[3]Division of Biosciences, University College London, Gower St, London, UK

[4]Eye Center, Albert-Ludwigs-University of Freiburg, Freiburg, Germany

*/[§]These authors contributed equally

[†]Present affiliation: Lee Kong Chian School of Medicine, Nanyang Technological University, Singapore

CORRESPONDING AUTHOR

Mahdad Noursadeghi (m.noursadeghi@ucl.ac.uk)

FINANCIAL SUPPORT:

This research was supported by a Gertrud-Kusen-Foundation fellowship (TL), the Rosetrees Trust, the Academy of Medical Sciences (SZ) and by NIHR Biomedical Research Centre funding to Moorfields Eye Hospital and UCL Institute of Ophthalmology, and by NIHR Biomedical Research Centre funding to University College London Hospitals and UCL.

ABSTRACT

Purpose. We sought to test the hypothesis that monocytes contribute to the immunopathogenesis of corneal allograft rejection and identify therapeutic targets to inhibit monocyte recruitment.

Methods. Monocytes and pro-inflammatory mediators within anterior chamber samples during corneal graft rejection were quantified by flow cytometry and multiplex protein assays. Lipopolysaccharide (LPS) or Interferon (IFN)γ stimulation of monocyte derived macrophages (MDM) was used to generate inflammatory conditioned media (CoM). Corneal endothelial viability was tested by nuclear counting, connexin 43 and propidium iodide staining. Chemokine and chemokine receptor expression in monocytes and MDM was assessed in microarray transcriptomic data. The role of chemokine pathways in monocyte migration across microvascular endothelium was tested *in vitro* by chemokine depletion or chemokine receptor inhibitors.

Results. Inflammatory monocytes were significantly enriched in anterior chamber samples within one week of the onset of symptoms of corneal graft rejection. MDM inflammatory CoM was cytopathic to transformed human corneal endothelia. This effect was also evident in endothelium of excised human cornea and increased by the presence of monocytes. Gene expression microarrays identified monocyte chemokine receptors and cognate chemokines in MDM inflammatory responses, which were also enriched in anterior chamber samples. Depletion of selected chemokines in MDM inflammatory CoM had no effect on monocyte transmigration across an endothelial blood-eye barrier but selective chemokine receptor inhibition reduced monocyte recruitment significantly.

Conclusions. We propose a role for inflammatory monocytes in endothelial cytotoxicity in corneal graft rejection. Therefore targeting monocyte recruitment offers a putative novel strategy to reduce donor endothelial cell injury in survival of human corneal allografts.

INTRODUCTION

Corneal transplantation remains the most commonly performed transplantation worldwide[1] and 25% of all corneal allografts fail within five years primarily as a result of immune mediated rejection[2]. The cellular requirements and the sequence of events in the effector component of the allogeneic response leading to endothelial corneal graft rejection are not fully understood and much of our information has been obtained from animal models. It is widely believed that $CD4^+$ T cells play an critical role in the rejection of rodent orthotopic corneal allografts[3-5] yet rejection can still occur in CD4 and interferon (IFN)γ KO mice[3, 6]. Furthermore, multiple and redundant effector mechanisms have been implicated in graft rejection[7] and may explain the poor outcomes in respect of rejection in corneal transplant recipients treated only with calcineurin antagonists which block T cell clonal expansion[8]. Several lines of evidence in rodent corneal transplantation suggest monocyte and macrophage involvement in the cell-mediated allogeneic response to transplanted cornea. Firstly, large numbers of macrophages are found in tissue sections at onset of corneal rejection in mouse and rat. At the earliest time points following the onset of corneal rejection in the rat, graft-infiltrating macrophages exceed T cells and NK cells[9], and in mice, MOMA-2^+ macrophages were reported among the earliest graft-infiltrating cells, before and after the onset of corneal rejection[10]. Secondly, local depletion of macrophages by subconjunctival administration with clodronate liposomes of corneal allotransplant recipients significantly prolonged corneal graft survival in treated rats using two different strain combinations[11, 12]. Local depletion of macrophages was found to downregulate infiltration of all alloreactive cell types, downregulate local and systemic cytotoxic lymphocyte responses and prevent the generation of antibodies[13]. Thirdly, earlier pilot investigation of immune cell populations in aqueous humour samples from the eye in patients at presentation with acute transplant rejection indicated a high proportion and selective recruitment of $CD14^+$ cells to the anterior chamber of the eye, likely to represent mononuclear phagocytic cells[14], corroborating an earlier report[15]. We sought to reconfirm and extend these data, investigate the mechanisms by which these cells may contribute to the mechanism of human corneal graft failure and investigate possible strategies to inhibit their recruitment across the blood-eye barrier, as a potential novel therapeutic intervention.

MATERIALS AND METHODS

Ethics

Ethics approval was provided by designated UK National Research Ethics Service committee for anterior chamber sampling from patients with acute corneal graft rejection and use of human corneal specimens in research (Research Ethics Committee reference: 11/LO/1294). Corneas, with healthy endothelium, were excised at surgery in keratoconus patients. Written informed consent was obtained from all participants. This study adhered to the tenets of the Declaration of Helsinki.

Aqueous humour analysis

Aqueous humour samples (100-200 µL), were obtained from ten patients presenting with corneal allograft rejection (Table 1). Diagnosis was confirmed by the finding in all patients of active anterior chamber inflammation and keratic precipitates on the donor corneal endothelium at slit-lamp biomicroscope examination. Control aqueous samples were obtained from nine patients undergoing routine cataract surgery (five male and four female; median age 57 range 3-85) without any other ocular disease. Samples were centrifuged at 400*g* for five minutes. The soluble fraction was collected and the cell pellet was resuspended in 100 µL phosphate buffered saline (PBS) with 0.5% bovine serum albumin (Sigma) and 0.01% sodium azide (Sigma). Total cell counts were enumerated with a hemocytometer and the cells were stained with directly conjugated fluorescent antibodies to CD14 (Becton Dickinson, clone M5E2) and CD16 (Becton Dickinson, clone 3G8). Immunostaining was quantified with a FACScalibur flow cytometer (Becton Dickinson) and FlowJo analysis software (version 9.4.3). Chemokine concentrations in these samples were measured using a flow cytometric multiplex bead assay kit (Milliplex, HCYTOMAG-60K).

Preparation of monocyte-derived macrophage conditioned media

Monocyte-derived macrophages (MDM) were prepared from human peripheral blood mononuclear cells (PBMC) as previously described[16]. After being allowed to differentiate for six days, the medium was changed to RPMI medium (Sigma) and 10% foetal calf serum (FCS, Biosera) with or without 100 ng/mL lipopolysaccharide (LPS) for 6 hours or 10 ng/mL IFNγ for 24 hours, using 1 mL media per 10^6 MDM. Conditioned media (CoM) from these cultures were then centrifuged at 10,000 *g* for five minutes and stored at -80°C. Residual LPS in LPS stimulated CoM was neutralised by addition of 10 µg/mL polymyxin B as described previously[16] and residual IFNγ was neutralised in IFNγ stimulated CoM by addition of 2 µg/mL blocking antibody to IFNγ. Effective functional neutralisation of LPS and IFNγ under these conditions was confirmed in monocyte transwell migration assays as described below, but without endothelial cells. We confirmed previous reports

that LPS inhibits monocyte migration in transwell assays and found that IFNγ had the same effect, which was reversed by addition of polymyxin B to neutralise LPS or antibody to neutralise IFNγ (Supplementary Figure 1). CoM for each condition was pooled from four separate MDM donors in order to minimise the effects of donor-donor variability.

Human corneal endothelial cell toxicity

The immortalised human corneal endothelial cell line (HCEC-B4G12, Ref- ACC 647, DCMZ, Germany)[17] was cultured in human endothelial serum free medium (Gibco) and 10 ng/ml FGF-2 (Gibco) in tissue culture plates pre-coated with 10 μg/mL laminin (Sigma Aldrich) and 10 mg/mL chondroitin sulphate (Sigma). At 70% confluence, the media was then changed to 10% CoM from LPS or IFNγ stimulated and unstimulated MDM before being washed with PBS and stained with calcein-AM (Sigma) and propidium iodide (PI, Sigma) as per manufacturer's instructions. Cellular fluorescence was imaged *in situ* on a Leica SPE inverted confocal microscope. Following removal of epithelium, freshly excised full thickness human cornea specimens were cut into quadrants at surgery with a diamond blade, placed in DME medium (Gibco) with 10% FCS overnight and then incubated for 24 hours with CoM from stimulated and unstimulated MDM. The corneas were then washed in PBS, fixed in 4% paraformaldehyde overnight, incubated in a blocking solution (PBS, 0.1M Lysine, 0.05% Triton X-100) for one hour, before immunostaining with a rabbit antibody for Connexin (Cx)43 (Sigma), fluorophore-conjugated secondary antibody and with a bis-benzamide nuclear counterstain. The stained cornea was washed in PBS and mounted in citifluor solution (Citifluor) and imaged using a Leica SPE confocal microscope. Sample identifiers were blinded for image analysis. Cx43 staining was quantified as previously described[18] and nuclear counting within multiple high power fields was performed manually.

Transwell migration assay across an endothelial barrier

Human cerebral microvascular endothelial cells (hCMEC/D3)[19] cells were obtained as kind gift from Dr PO Couraud (Institut Cochin, Paris, France). These were cultured in endothelial growth medium-2 (EGM-2, Lonza) supplemented with 5% FCS, 1% penicillin-streptomycin (Gibco), 1.4 μM hydrocortisone (Sigma), 5 μg/ml ascorbic acid (Sigma), 1% chemically defined lipid concentrate (Gibco), 10mM HEPES (Gibco) and 1 ng/ml human fibroblast growth factor (Sigma). Cells were seeded at $5x10^4$ cells/cm^2 on the apical side of 0.33 cm^2 polycarbonate transwell inserts (Corning No. 3421, 6.5 mm diameter, 5.0 μm pores) pre-coated with Cultrex rat type 1 collagen 50 μg/ml (R&D Systems). To form a monolayer hCMEC/D3 cells were maintained in culture for six days with media changes after three and six days[19] and supplemented with 10mM lithium chloride (Santa Cruz Biotechnology) for the entire culture period to generate tight junctions[20, 21] confirmed by transendothelial electrical resistance (TEER) measurements using an electrical Volt-Ohm-Meter (EVOM-2,

World Precision Instruments). After six days, the transwells were then transferred into wells containing 10% stimulated or unstimulated CoM for 24 hours. Cellular transmigration across the endothelial barrier was assessed by addition of $5x10^5$ peripheral blood mononuclear cells (PBMC) obtained from healthy volunteers into the upper chamber of the transwell for three hours at 37°C, before collecting cells in the lower chamber. This cell suspension was then stained for CD14 and CD16 and enumerated by flow cytometry using Flow-CheckTM polystyrol fluorospheres (Beckman Coulter) to standardise cell counting. Monocytes and lymphocytes were discriminated by light scatter properties and CD14/CD16 staining. Transmigration of cells into the lower chamber was expressed as a proportion of the input.

Chemokine and chemokine receptor expression data

Data on normalised chemokine receptor expression in monocytes and chemokine expression in LPS or IFNγ-stimulated MDM was obtained from the European Bioinformatics Institute data repository (www.ebi.ac.uk/arrayexpress/) using accession numbers E-TABM-1206 and E-MEXP-2032. A network of interacting chemokines and chemokine receptors was adopted from the KEGG cytokine-cytokine receptor interaction reference pathway (www.genome.jp/kegg/kegg2.html, map0460) and constructed in Gephi graph visualization software (version 0.8.2). The transcriptomes of hCMEC/D3 cells after 24 hour incubation with CoM from unstimulated MDM and LPS-stimulated MDM with PMB were also compared by genome-wide expression arrays. Total RNA was purified from cell lysates collected in RLT buffer (Qiagen) using the RNeasy Mini kit (Qiagen). Samples were processed for Agilent microarrays as previously described[22] and loess normalized data wereanalysed using theTM4 microarray software suite MeV (version 4.9). Pathway enrichment analysis of differentially expressed gene lists was performed using the online bioinformatics tools InnateDB[23] and Ingenuity Pathway Analysis (http://www.ingenuity.com/). Microarray data are available from the EBI Array Express repository (http://www.ebi.ac.uk/arrayexpress/) under accession no E-MTAB-3692.

Chemokine depletion and chemokine receptor targeting

To deplete single or a combination of different monocyte chemotactic chemokines, biotinylated anti-human antibody against CCL2, CCL3, CCL4, and CCL8 were added at a concentration of 5 µg/mL to the different CoM. The biotinylated antibodies were incubated with the CoM for one hour at room temperature before addition of magnetic streptavidin beads (Dynabeads MyOne Streptavidin T1, Life Technologies) using 10^9 beads/mL. These were incubated for one hour with the CoM before removing the beads magnetically. Successful depletion was confirmed by ELISA using paired capture and detection antiboides for each chemokine (eBioscience) according to manufacturer's instructions and analysed using a Multiskan absorbance plate reader (Thermo Labsystems). For chemokine receptor targeting, $5x10^6$ cells/mL PBMC were incubated

with inhibitors of CCR2 (RS 504393 or BMS CCR2 22, both from Tocris), CCR5 (Maraviroc, Tocris), or CXCR4 (AMD 3465 hexahydrobromide, Tocris), used at 10 nM, for 30 minutes.

Statistical analysis

Data were analysed using Graphpad Prism software Version 5. The Mann-Whitney U- or t-tests were used to test significance. Values of $p<0.05$ were defined as statistically significant.

RESULTS:

Enrichment of inflammatory monocytes in the aqueous humour of patients with acute corneal graft rejection.

Samples of aqueous humour from the anterior chamber were obtained from ten patients with endothelial corneal allograft rejection. The demographic characteristics, primary diagnosis leading to corneal transplantation, number of previous transplants and previous episodes of allograft rejection, and corticosteroid therapy at time of rejection are summarised in Table 2. Total cell counts in the aqueous humour samples revealed that a cellular infiltrate was only detectable in aqueous humour samples from patients presenting within seven days of the onset of symptoms (Figure 1A), irrespective of concomitant corticosteroid treatment (Supplementary Figure 2). Within these samples, we confirmed our previous observation[14] that $CD14^+$ cells were significantly enriched in the aqueous humour compared to peripheral blood (Figure 1B). We extended these data to show that the enrichment of $CD14^+$ cells was entirely due to $CD14^{hi}CD16^{low}$ classical inflammatory monocytes, known to be recruited to inflammatory foci (Figure 1C).

Monocyte-derived macrophages generate inflammatory mediators that deplete corneal endothelial cells.

Classical inflammatory monocytes are extremely short-lived with a half-life of less than 24 hours[24], unless they differentiate into macrophages as a result of environmental signals. Therefore, we reasoned that if monocyte recruitment to the eye contributes to the pathogenesis of corneal transplant rejection, inflammatory mediators generated by monocyte-derived macrophages (MDM) may cause donor corneal endothelial cytotoxicity and depletion. Macrophages produce inflammatory mediators in response to innate immune danger signals or interferon (IFN)γ production by lymphocytes. We therefore modelled macrophage inflammatory responses by stimulating MDM with either lipopolysaccharide (LPS) or recombinant IFNγ, and we pooled conditioned media (CoM) from stimulated and unstimulated MDM cultures from multiple experiments in order to minimise the confounding of donor to donor variability. In order to focus on the role of the MDM-derived inflammatory response in downstream experiments with these CoM, we neutralised LPS or IFNγ activity by addition of polymyxin B or blocking antibody to IFNγ to the relevant samples. We first assessed the effect of MDM CoM on survival of an immortalized human endothelial cell line and found that CoM from LPS-stimulated MDM induced significant endothelial cell death, indicated by propidium iodide (PI) staining (Figure 2A). In order to extend these observations further, we then evaluated the effect of MDM CoM on endothelial cells in excised corneal specimens *ex vivo* by counting the number of nuclei in the endothelial layer and by quantifying

expression of the gap junction protein connexin (Cx)43 as a surrogate for the integrity of the endothelial layer. In keeping with the effect on the corneal endothelial cell line, we found that CoM from LPS-stimulated MDM induced significant loss of cells of the corneal endothelium and reduction of detectable Cx43 immunostaining (Figure 2B-D). In these experiments, we also found depletion of endothelial cells and loss of Cx43 staining as a result of incubation with CoM from IFNγ-stimulated MDM, albeit to a lesser degree than LPS-stimulated CoM (Figure 2B-D). In addition, we found that the presence of monocytes in this experimental model significantly increased the cytopathic effect of LPS-stimulated CoM as measured by reduction in Cx43 staining (Figure 3).

Identification of putative targets to modulate monocyte recruitment.

Our data implicate recruitment of functionally active monocytes in the pathogenesis of corneal allograft rejection. Therapeutic targeting of monocyte recruitment may therefore provide a novel strategy to limit injury to donor corneal endothelium. Given the importance of chemokine pathways to mediate cell-specific recruitment, we sought to identify the principal chemokine or chemokine receptors that control human monocyte recruitment to inflammatory foci. To do this we cross-referenced previously published transcriptomic data for chemokine receptor expression in human monocytes[25] (Figure 4A), chemokine expression by MDM stimulated with LPS or IFNγ[26] (Figure 4B) with established networks of chemokine and chemokine receptor interactions (Figure 4C). This analysis identified eight chemokines (CCL2, CCL3, CCL4, CCL5, CCL7, CCL8, CCL13 and CCL18) and the most highly expressed chemokine receptors (CCR1, CCR2 and CCR5) which may participate in amplification of monocyte recruitment to putative inflammatory foci. Importantly, using a multiplex protein assay which included reagents for CCL2, CCL3 and CCL4, we found that each of these chemokines were also detectable at significantly greater levels in anterior chamber samples from patients with acute corneal graft rejection within seven days of symptom onset, compared to samples from patients with greater than seven days symptoms or samples from control patients (Figure 5). These data highlight the most likely monocyte chemokine pathways involved in monocyte recruitment in acute corneal graft rejection.

Macrophage inflammatory responses drive monocyte recruitment across a blood-eye barrier

Next, we developed an experimental model for monocyte transmigration across the blood-eye barrier in order to test the hypothesis that the chemokine pathways described above were necessary for monocyte recruitment and could therefore be targeted to effectively reduce monocyte recruitment in corneal allograft rejection. We used a well-characterised human endothelial cell line derived from brain microvasculature to establish an endothelial barrier with tight junctions in transwells (Figure 6A-B). Inflammatory CoM from LPS or IFNγ-stimulated MDM added to the bottom compartment of the transwell apparatus induced significantly greater monocyte transmigration from top to bottom compartment (Figure 6A and 6C). We used unfractionated PBMC

in order to compare monocyte and lymphocyte recruitment. Consistent with our *in vivo* finding that monocytes are enriched in the anterior chamber of patients with acute corneal graft rejection, we found significantly greater transmigration of monocytes compared to lymphocytes in this *in vitro* model (Figure 6C).

Chemokine receptor targeting to attenuate monocyte transmigration across a blood-eye barrier.

In order to reduce monocyte recruitment in corneal graft rejection to a functionally significant degree, we reasoned that it might be possible to target either the chemokines or chemokine receptors. To test the effect of chemokine targeting we depleted LPS-stimulated MDM CoM of selected chemokines identified in the experiments above individually, or all of these chemokines together. We found no attenuation of monocyte transmigration in the endothelial blood-eye barrier model (Figure 7A). In response to pro-inflammatory stimuli, endothelial cells upregulate cell adhesion molecules and chemokines that contribute to leukocyte recruitment[27-29]. Accordingly, genome-wide transcriptional responses in hCMEC/D3 cells to CoM from LPS-stimulated MDM revealed upregulation of canonical cell adhesion molecules involved in leukocyte adhesion and diapedesis, and significant enrichment of secreted products with chemotactic activity (Supplementary Figure 3) including CCL2, CCL5, CCL7 and CCL8 (Figure 7B), thereby supporting monocyte recruitment despite depletion of these chemokines in the CoM from LPS-stimulated MDM. Therefore we considered targeting their cognate chemokine receptors instead. A number of small molecules inhibitors of the chemokine receptors CCR2 and CCR5 have already been evaluated in clinical trials. We therefore tested the effect of small molecule inhibitors of these chemokine receptors on monocyte transmigration. We found that targeting CCR2 with inhibitory molecules significantly attenuated monocyte recruitment (Figure 7C). A CCR5 inhibitor also showed the same effect but did not reach statistical significance in four experimental replicates. In contrast a small molecule targeting CXCR4 had no effect on monocyte recruitment (Figure 7C). CXR4 is expressed by monocytes (Figure 4A) but its ligand, CXCL12 (Figure 3C) was not upregulated in LPS or IFNγ-stimulated MDM (Figure 4B),. Of note, CCR2 expression and function are known to be downregulated as monocytes are differentiated to macrophages[30], although some subsets of macrophages may retain higher CCR2 expression[31]. This is also reflected in our analysis of the transcriptomes of monocytes and MDM (Supplementary Figure 4), even after MDM stimulation with LPS or IFNγ, and is consistent with the hypothesis CCR2 has a specific role in tissue recruitment of circulating monocytes.

DISCUSSION

In the present manuscript, we show three lines of evidence to support a role for monocytes in corneal rejection. Firstly, classical inflammatory monocytes are specifically enriched in anterior chamber specimens from patients with acute corneal rejection. Secondly, the pro-inflammatory mediators of monocyte derived cells are sufficient to induce cell death of a human corneal endothelial cell line in vitro and death of primary human corneal endothelial cells in corneal buttons ex vivo. Thirdly, the addition of monocytes to proinflammatory mediators significantly enhances corneal endothelial cell death. $CD14^{hi}$ monocytes comprise about 10% of PBMC in health. Therefore, the finding that 40-50% of cells within aqueous humour samples of patients at the time of acute corneal allograft rejection are monocytes clearly indicates selective recruitment, further supported by the finding of elevated levels of chemokines CCL2, CCL3 and CCL4, known to be chemoattractant for monocytes. These were almost entirely $CD16^{low}$ cells, which is the predominant monocyte subset to be recruited to inflammatory foci and suggests that these cells are likely to be functionally active in the allogeneic tissue injury response. It is of note that the cellular infiltrate was only evident in patients with symptoms for less than seven days, indicating that these specimens were examined shortly following the onset of the effector phase of the allogeneic response. Of note, this observation was not confounded by presence or absence of corticosteroid treatment, albeit our sample size was too small for statistically robust subgroup analysis. Additional comparisons in immune correlates of alternative corneal pathologies would be necessary to test the specificity of our findings for acute corneal allograft rejection.

Monocytes typically survive less than 24 hours, or differentiate into tissue resident macrophages and dendritic cells[24]. We speculate that monocyte recruitment to the anterior chamber represents one of the earliest events in the effector phase of corneal allograft rejection and is associated with monocyte differentiation. Hence, the absence of cells later than seven days following the onset of transplant rejection symptoms may reflect the transition to macrophages that migrate from the anterior chamber or adhere to the transplant surface, as suggested by data from rodent models[9]. Our study does not address the question of the initial inflammatory trigger that stimulates monocyte recruitment in the first instance. The intersection of coagulation pathways with inflammation, and inflammatory responses that arise from so-called danger associated molecular patterns suggest tissue injury may lead to innate immune responses that augment adaptive immune responses to allogeneic antigens[32]. In corneal transplantation the mechanical trauma of surgery may cause significant tissue damage, leading to activation of resident antigen-presenting cells and enhanced immunogenicity, in keeping with the danger model proposed by Matzinger[33].

Macrophage infiltration has also long been recognised as a hallmark of acute allograft rejection after heart transplantation[34], and a number of studies suggest that macrophages can promote acute renal allograft rejection[35-37]. The functional consequence of modulating macrophage function in corneal transplantation was most directly shown by prolongation of rat corneal allograft survival following depletion of conjunctival macrophages with clodronate liposomes[13]. One component of the present study was to assess whether inflammatory responses from MDM may contribute to loss of donor corneal function in rejection by causing endothelial cell death and thereby compromising the transparency of donor cornea. In two separate models we found CoM from LPS stimulated MDM, and to a lesser extent IFNγ-stimulated MDM caused significant corneal endothelial cell loss. Furthermore, monocytes had an additional direct cytotoxic effect on human corneal endothelium *ex vivo* but only in the context of inflammation. This suggests therefore that the inflammatory cellular microenvironment either drives further pro-inflammtory cytokine release and subsequent cytotoxicity; in keeping with published evidence showing inflammatory cytokines to promote endothelial cell apoptosis[38-41] or that the monocytes themselves become activated and release tissue destructive lysosomal enzymes or free radicals that are directly cytotoxic[42-44]. Further characterisation of the fate and phenotype of the monocyte derived macrophages that accumulate during corneal rejection is necessary to test these hypotheses. Due to the limited availability and volume of human aqueous humour sampling, this was not possible in the present study, but requires renewed assessments of tissue specimens from rejected corneal allografts or further experimental studies in animal models. In addition, the mechanism of corneal endothelial cell death is not addressed in our current experiments, but specific cell death pathways, including apoptosis, pyroptosis and necroptosis all intersect with inflammatory responses and may therefore be implicated. Elucidating which of these pathways makes the greatest contribution will be important in future studies in order to identify targets to inhibit corneal endothelial cell death.

Our data suggest a rationale for therapeutic targeting of monocyte recruitment and we investigated targeting of the monocyte chemotaxis. Cross-reacting specificities of chemokines and chemokine receptors generate a network with potential for significant functional redundancy that may undermine the use of specific inhibitors. We cross-referenced chemokine receptor expression in monocytes and chemokine production in stimulated MDM with existing databases for chemokine pathways in order to identify those that may contribute to inflammatory monocyte recruitment in our model. Our experimental model simulated changes to chemokine levels associated with acute human corneal graft rejection. We therefore adopted an experimental system in which we could test the role of selected chemokine or chemokine receptors for monocyte migration across endothelial cells which exhibit the tight junction features of the blood-aqueous or blood-brain barrier. Given the

functional redundancy within the chemokine network, we were not surprised to find that depletion of individual chemokines in this system had no significant effect on monocyte migration. It was more surprising that depletion of several chemokines that we predicted may play a role also had no effect on chemokine transmigration. However, we found that the endothelial cells modelling the blood-brain barrier also produced these chemokines and can therefore drive monocyte recruitment in response to paracrine activation by macrophages. Therefore, we tested the effect of targeting key monocyte chemokine receptors instead, using CCR2 and CCR5 small molecule inhibitors which have shown some efficacy in preclinical and clinical models of rheumatoid disease[45, 46]. Blockade of CCR2, which interacts with CCL2, CCL7, CCL8 and CCL13 did result in partial inhibition of monocyte transmigration, suggesting that this receptor at least plays a non-redundant role in recruitment of inflammatory monocytes. Additional sampling and analysis of the humoral and cellular components enriched in acute corneal rejection is needed to overcome the limitations of the small aqueous humour sample size in the present study. Nonetheless, our findings add to the evidence for the role of monocyte recruitment early on in the effector phase of corneal transplant rejection and highlights the potential for chemokine receptor blockade to reduce donor endothelial cell injury in rejection. *In vivo* studies will be required to examine the efficacy of this novel immunomodulatory approach in attenuating allogenic injury to donor endothelium and prolonging human corneal transplant survival. Of note, experimental corneal rejection was ameliorated in mice with targeted deletions of CCR1, but not in mice deleted for CCR2 and CCL3[46]. Although total mononuclear cell recruitment to the site of rejection was attenuated in CCR1 deficient mice, monocyte recruitment specifically was not evaluated and cellular recruitment in CCR2/CCL3 deficient mice was not reported. Therefore genetic and pharmaceutical targeting of chemokine recptors in mouse models merit further evaluation in order to pave the way for first in man clinical studies.

REFERENCES

1. Report of the organ transplant panel. Corneal transplantation. Council on Scientific Affairs. *JAMA* 1988;259:719-722.

2. Williams KA, Lowe M, Bartlett C, Kelly TL, Coster DJ, All C. Risk factors for human corneal graft failure within the Australian corneal graft registry. *Transplantation* 2008;86:1720-1724.

3. Yamada J, Kurimoto I, Streilein JW. Role of CD4+ T cells in immunobiology of orthotopic corneal transplants in mice. *Invest Ophthalmol Vis Sci* 1999;40:2614-2621.

4. He YG, Ross J, Niederkorn JY. Promotion of murine orthotopic corneal allograft survival by systemic administration of anti-CD4 monoclonal antibody. *Invest Ophthalmol Vis Sci* 1991;32:2723-2728.

5. Ayliffe W, Alam Y, Bell EB, McLeod D, Hutchinson IV. Prolongation of rat corneal graft survival by treatment with anti-CD4 monoclonal antibody. *Br J Ophthalmol* 1992;76:602-606.

6. Niederkorn JY, Stevens C, Mellon J, Mayhew E. CD4+ T-cell-independent rejection of corneal allografts. *Transplantation* 2006;81:1171-1178.

7. Niederkorn JY. Immune mechanisms of corneal allograft rejection. *Curr Eye Res* 2007;32:1005-1016.

8. Chatel MA, Larkin DF. Sirolimus and mycophenolate as combination prophylaxis in corneal transplant recipients at high rejection risk. *Am J Ophthalmol* 2010;150:179-184.

9. Larkin DF, Calder VL, Lightman SL. Identification and characterization of cells infiltrating the graft and aqueous humour in rat corneal allograft rejection. *Clin Exper Immunol* 1997;107:381-391.

10. Kuffova L, Lumsden L, Vesela V, et al. Kinetics of leukocyte and myeloid cell traffic in the murine corneal allograft response. *Transplantation* 2001;72:1292-1298.

11. Van der Veen G, Broersma L, Dijkstra CD, Van Rooijen N, Van Rij G, Van der Gaag R. Prevention of corneal allograft rejection in rats treated with subconjunctival injections of liposomes containing dichloromethylene diphosphonate. *Invest Ophthalmol Vis Sci* 1994;35:3505-3515.

12. Slegers TP, Broersma L, van Rooijen N, Hooymans JM, van Rij G, van der Gaag R. Macrophages play a role in the early phase of corneal allograft rejection in rats. *Transplantation* 2004;77:1641-1646.

13. Slegers TP, Torres PF, Broersma L, van Rooijen N, van Rij G, van der Gaag R. Effect of macrophage depletion on immune effector mechanisms during corneal allograft rejection in rats. *Invest Ophthalmol Vis Sci* 2000;41:2239-2247.

14. Flynn TH, Mitchison NA, Ono SJ, Larkin DF. Aqueous humor alloreactive cell phenotypes, cytokines and chemokines in corneal allograft rejection. *Am J Transplant* 2008;8:1537-1543.

15. Reinhard T, Bocking A, Pomjanski N, Sundmacher R. Immune cells in the anterior chamber of patients with immune reactions after penetrating keratoplasty. *Cornea* 2002;21:56-61.

16. Noursadeghi M, Tsang J, Haustein T, Miller RF, Chain BM, Katz DR. Quantitative imaging assay for NF-kappaB nuclear translocation in primary human macrophages. *J Immunol Methods* 2008;329:194-200.

17. Valtink M, Gruschwitz R, Funk RH, Engelmann K. Two clonal cell lines of immortalized human corneal endothelial cells show either differentiated or precursor cell characteristics. *Cells, tissues, organs* 2008;187:286-294.

18. Wang CM, Lincoln J, Cook JE, Becker DL. Abnormal connexin expression underlies delayed wound healing in diabetic skin. *Diabetes* 2007;56:2809-2817.

19. Hatherell K, Couraud PO, Romero IA, Weksler B, Pilkington GJ. Development of a three-dimensional, all-human in vitro model of the blood-brain barrier using mono-, co-, and tri-cultivation Transwell models. *J Neurosci Methods* 2011;199:223-229.

20. Liebner S, Corada M, Bangsow T, et al. Wnt/beta-catenin signaling controls development of the blood-brain barrier. *J Cell Biol* 2008;183:409-417.

21. Ramirez SH, Fan S, Zhang M, et al. Inhibition of glycogen synthase kinase 3beta (GSK3beta) decreases inflammatory responses in brain endothelial cells. *American J Pathol* 2010;176:881-892.

22. Chain B, Bowen H, Hammond J, et al. Error, reproducibility and sensitivity: a pipeline for data processing of Agilent oligonucleotide expression arrays. *BMC Bioinformatics* 2010;11:344.

23. Breuer K, Foroushani AK, Laird MR, et al. InnateDB: systems biology of innate immunity and beyond--recent updates and continuing curation. *Nucleic Acids Res* 2013;41:D1228-1233.

24. Varol C, Yona S, Jung S. Origins and tissue-context-dependent fates of blood monocytes. *Immunol Cell Biol* 2009;87:30-38.

25. Tomlinson GS, Booth H, Petit SJ, et al. Adherent human alveolar macrophages exhibit a transient pro-inflammatory profile that confounds responses to innate immune stimulation. *PloS One* 2012;7:e40348.

26. Tsang J, Chain BM, Miller RF, et al. HIV-1 infection of macrophages is dependent on evasion of innate immune cellular activation. *AIDS* 2009;23:2255-2263.

27. Hillyer P, Male D. Expression of chemokines on the surface of different human endothelia. *Immunol Cell Biol* 2005;83:375-382.

28. Lin CF, Chiu SC, Hsiao YL, et al. Expression of cytokine, chemokine, and adhesion molecules during endothelial cell activation induced by antibodies against dengue virus nonstructural protein 1. *J Immunol* 2005;174:395-403.

29. Brown Z, Gerritsen ME, Carley WW, Strieter RM, Kunkel SL, Westwick J. Chemokine gene expression and secretion by cytokine-activated human microvascular endothelial cells. Differential regulation of monocyte chemoattractant protein-1 and interleukin-8 in response to interferon-gamma. *Am J Pathol* 1994;145:913-921.

30. Fantuzzi L, Borghi P, Ciolli V, Pavlakis G, Belardelli F, Gessani S. Loss of CCR2 expression and functional response to monocyte chemotactic protein (MCP-1) during the differentiation of human monocytes: role of secreted MCP-1 in the regulation of the chemotactic response. *Blood* 1999;94:875-883.

31. LaRosa DF, Rahman AH, Turka LA. The innate immune system in allograft rejection and tolerance. *J Immunol* 2007;178:7503-7509.

32. Matzinger P. The danger model: a renewed sense of self. *Science* 2002;296:301-305.

33. Wu YL, Ye Q, Eytan DF, et al. Magnetic resonance imaging investigation of macrophages in acute cardiac allograft rejection after heart transplantation. *Circ Cardiovasc Imaging* 2013;6:965-973.

34. Trpkov K, Campbell P, Pazderka F, Cockfield S, Solez K, Halloran PF. Pathologic features of acute renal allograft rejection associated with donor-specific antibody, Analysis using the Banff grading schema. *Transplantation* 1996;61:1586-1592.

35. Mauiyyedi S, Crespo M, Collins AB, et al. Acute humoral rejection in kidney transplantation: II. Morphology, immunopathology, and pathologic classification. *J Am Soc Nephrol* 2002;13:779-787.

36. Solez K, Colvin RB, Racusen LC, et al. Banff 07 classification of renal allograft pathology: updates and future directions. *Am J Transplant* 2008;8:753-760.

37. Sagoo P, Chan G, Larkin DF, George AJ. Inflammatory cytokines induce apoptosis of corneal endothelium through nitric oxide. *Invest Ophthalmol Vis Sci* 2004;45:3964-3973.

38. Kildahl-Andersen O, Espevik T, Nissen-Meyer J. IFN-gamma-induced production of monocyte cytotoxic factor. *Cell Immunol* 1985;95:392-406.

39. Kildahl-Andersen O, Nissen-Meyer J. Production and characterization of cytostatic protein factors released from human monocytes during exposure to lipopolysaccharide and muramyl dipeptide. *Cell Immunol* 1985;93:375-386.

40. Philip R, Epstein LB. Tumour necrosis factor as immunomodulator and mediator of monocyte cytotoxicity induced by itself, gamma-interferon and interleukin-1. *Nature* 1986;323:86-89.

41. Cathcart MK, Morel DW, Chisolm GM, 3rd. Monocytes and neutrophils oxidize low density lipoprotein making it cytotoxic. *Journal of leukocyte biology* 1985;38:341-350.

42. Mene P, Pugliese F, Cinotti GA. Adhesion of U-937 monocytes induces cytotoxic damage and subsequent proliferation of cultured human mesangial cells. *Kidney Int* 1996;50:417-423.

43. Jaattela M, Wissing D. Heat-shock proteins protect cells from monocyte cytotoxicity: possible mechanism of self-protection. *J Exp Med* 1993;177:231-236.

44. van Kuijk AW, Vergunst CE, Gerlag DM, et al. CCR5 blockade in rheumatoid arthritis: a randomised, double-blind, placebo-controlled clinical trial. *Annals of the rheumatic diseases* 2010;69:2013-2016.

45. Vergunst CE, Gerlag DM, Lopatinskaya L, et al. Modulation of CCR2 in rheumatoid arthritis: a double-blind, randomized, placebo-controlled clinical trial. *Arthritis and rheumatism* 2008;58:1931-1939.

46. Hamrah P, Yamagami S, Liu Y, et al. Deletion of the chemokine receptor CCR1 prolongs corneal allograft survival. *Invest Ophthalmol Vis Sci* 2007;48:1228-1236.

TABLE 1

Inclusion criteria	Exclusion criteria
Patients who have had a penetrating keratoplasty and have been diagnosed with endothelial rejection by one or more of the following: • Endothelial rejection line • Graft KP with aqueous cells • Visible aqueous cells with graft oedema in a previously clear graft.	Patients with a history of HSV keratitis in that eye

TABLE 2

Patient	Age	Sex	Primary corneal diagnosis	No. of previous transplants	Previous rejection episodes	Duration of symptoms (days) prior to sample collection	Time after transplant (months)	Prior topical steroids
1	42	M	Microbial keratitis	0	No	2	11	No
2	53	F	Ectasia post LASIK	3	Yes	2	1	Yes
3	23	F	Keratoconus	0	No	14	9	Yes
4	39	M	Keratoconus	1	Yes	2	31	Yes
5	42	M	Keratoconus	0	No	10	18	Yes
6	86	M	Fuchs disease	0	No	17	16	No
7	48	M	Keratoconus	0	No	7	27	Yes
8	90	M	Pseudophakic bullous keratopathy	0	No	14	12	No
9	52	M	Keratoconus	0	No	14	17	No
10	26	M	Macular dystrophy	0	Yes	1	12	Yes

FIGURE LEGENDS

Figure 1

(A) Total cell counts in aqueous humour (AH) samples were compared in patients with more or less than seven days symptoms of corneal allograft rejection. In patients for whom a cellular infiltrate was evident (n = 5), the proportion of all $CD14^+$ cells **(B)** and monocyte subsets discriminated by the combination of CD14 and CD16 staining **(C)** was compared in AH and contemporaneous PBMC samples. The inset dot plot shows the gating strategy used to quantify each of monocyte subsets indicated. *****indicates statistically significant differences (p<0.05, Mann-Whitney U-test). Measurements for individual patient samples are shown in A and summarised as median ±IQR in B and C.

Figure 2

(A) Propidium iodide and calcein staining in a human corneal endothelial cell line incubated with CoM from unstimulated (control) and LPS or IFNγ stimulated MDM, was visualised by immunofuoresence microscopy at 30 and 690 minutes. **(B)** Cx43 and nuclear staining in the endothelial layer of human cornea specimens incubated overnight with CoM from unstimulated and LPS or IFNγ stimulated MDM was visualised by confocal microscopy. Quantitaion of numbers of visible nuclei and positive Cx43 staining per high power field is summarised from four separate experiments **(C-D)**. *****indicates statistically significant differences (p<0.05, Mann-Whitney U-test). Bars represent median ±IQR. Fluorescence images are representative of four separate experiments in each case.

Figure 3

(A) Cx43 and nuclear staining (DAPI) in the endothelial layer of human cornea specimens incubated *ex vivo* for 24 hours with CoM from unstimulated (Control) and LPS or IFNγ stimulated MDM followed by an overnight incubation with CD14 selected human monocytes (Mo) was visualised by confocal microscopy. Quantitation of numbers of visible nuclei and positive Cx43 staining per high power field is summarised from four separate experiments **(B-C)**. *****indicates statistically significant differences (p<0.05, Mann-Whitney U-test). Bars represent mean ± SEM. Fluorescence images are representative of four separate experiments.

Figure 4

(A) Relative mRNA expression of chemokine receptors by peripheral blood monocytes from separate healthy volunteer donors and **(B)** mean fold change of chemokine transcript levels in LPS or IFNγ-stimulated MDM, are derived from previously published data sets. **(C)** A network diagram of known chemokine receptor-ligand

interactions for all the chemokine receptors expressed in A, above the median normalised expression level of 8 (Log_2), in which the size of the nodes is proportional to the number of interactions. Interactions between chemokine receptors (yellow nodes) in this network and chemokines (red nodes) which are upregulated in LPS or IFNγ-stimulated MDM are highlighted.

Figure 5

Comparison of selected chemokine concentrations (CCL2, CCL3 and CCL4) in aqueous humour samples from patients with corneal allograft rejection grouped by duration of symptoms (more or less than one week duration), and samples from control patients undergoing cataract surgery. Measurements from individual patient samples and the median of each group are indicated. *****indicates statistically significant differences (p<0.05, Mann-Whitney U-test).

Figure 6

(A) Schematic representation of the transwell model to evaluate PBMC transmigration across a blood-eye barrier. The hCMEC/D3 cell line is cultured in transwell and allowed to form tight junctions, followed by incubation in CoM from stimulated and unstimulated MDM in the lower chamber and addition of unfractionated PBMC in the top chamber. **(B)** Measurement of trans endothelial electrical resistance (TEER) across hCMEC/D3 cells in culture with and without Lithium supplementation to encourage tight junction formation. **(C)** Quantiation of $CD14^+$ (monocytes) and $CD14^-$ (lymphocytes) fraction of PBMC migrating through the hCMEC/D3 barrier as proportion of the total PBMC loaded into the top chamber, in response to each of the MDM CoM indicated in the lower chamber. In B, bars represent mean ±SEM of at least 10 separate measurements. In C, bars represent mean ±SEM of six separate experiments. *****indicates statistically significant differences (p<0.05, t-test).

Figure 7

(A) Monocyte transmigration across hCMEC/D3 cells incubated with CoM from LPS stimulated MDM was compared with and without depletion of selected chemokines from the CoM reflected in the final concentration of the each of the chemokines indicated in the heat map panel. **(B)** Gene expression heat map of chemokines upregulated in hCMEC/D3 cells incubated with CoM from LPS stimulated MDM compared to CoM from unstimulated MDM in four independent experiments. **(C)** Monocyte transmigration across hCMEC/D3 cells incubated with CoM from LPS stimulated MDM was compared in the presence and absence of small molecule inhibitors of the chemokine receptors indicated. Data bars represent mean±SEM of four separate experiments in each case. *****indicates statistically significant differences (p<0.05,t-test).

Figure 1

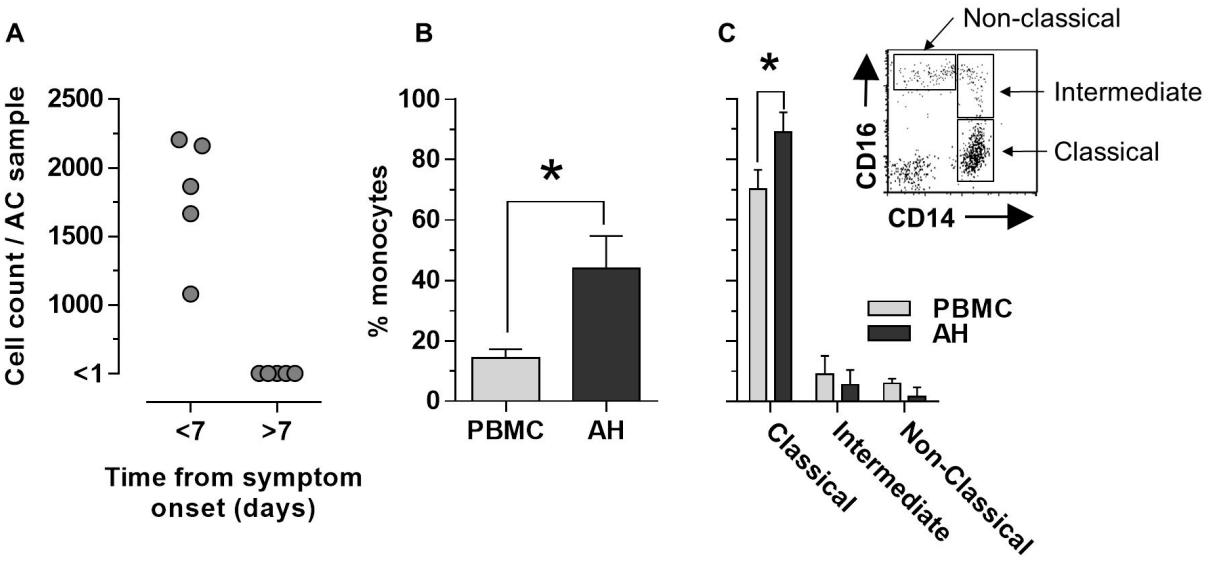
A
Cell count / AC sample
2500
2000
1500
1000
<1
<7
>7
Time from symptom onset (days)
B
% monocytes
100
80
60
40
20
0
*
PBMC
AH
C
*
Non-classical
Intermediate
Classical
CD16
CD14
PBMC
AH
Classical
Intermediate
Non-Classical

Figure 2

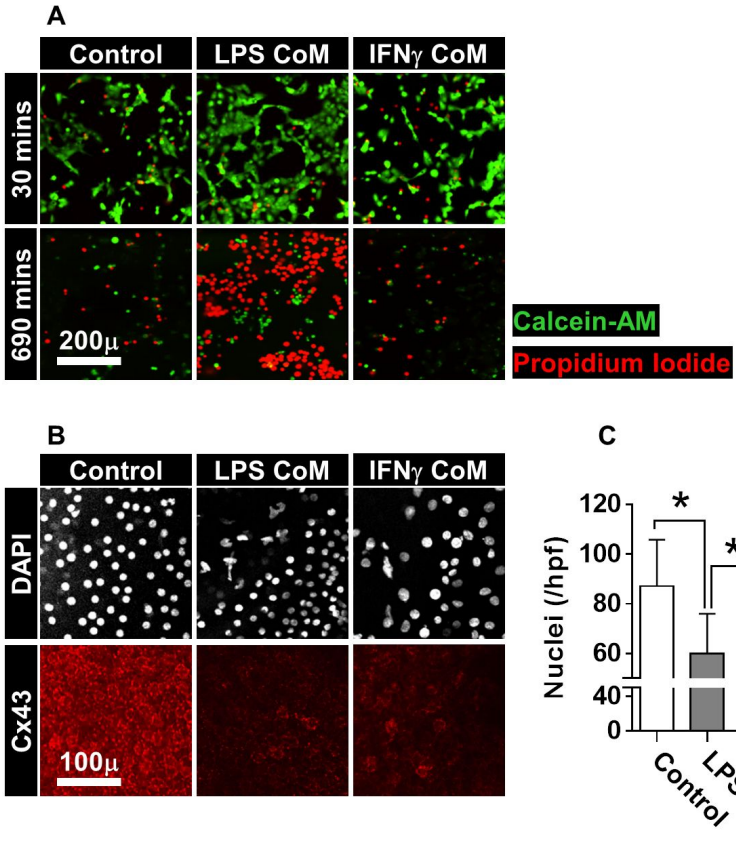
A
Control
LPS CoM
IFNγ CoM
30 mins
690 mins
200μ
Calcein-AM
Propidium Iodide
B
Control
LPS CoM
IFNγ CoM
DAPI
Cx43
100μ
C
Nuclei (/hpf)
120
100
80
60
40
0
*
*
Control
LPS CoM
IFNγ CoM
D
CX43 (pixel ct)
20
15
10
5
0
*
*
Control
LPS CoM
IFNγ CoM

Figure 3

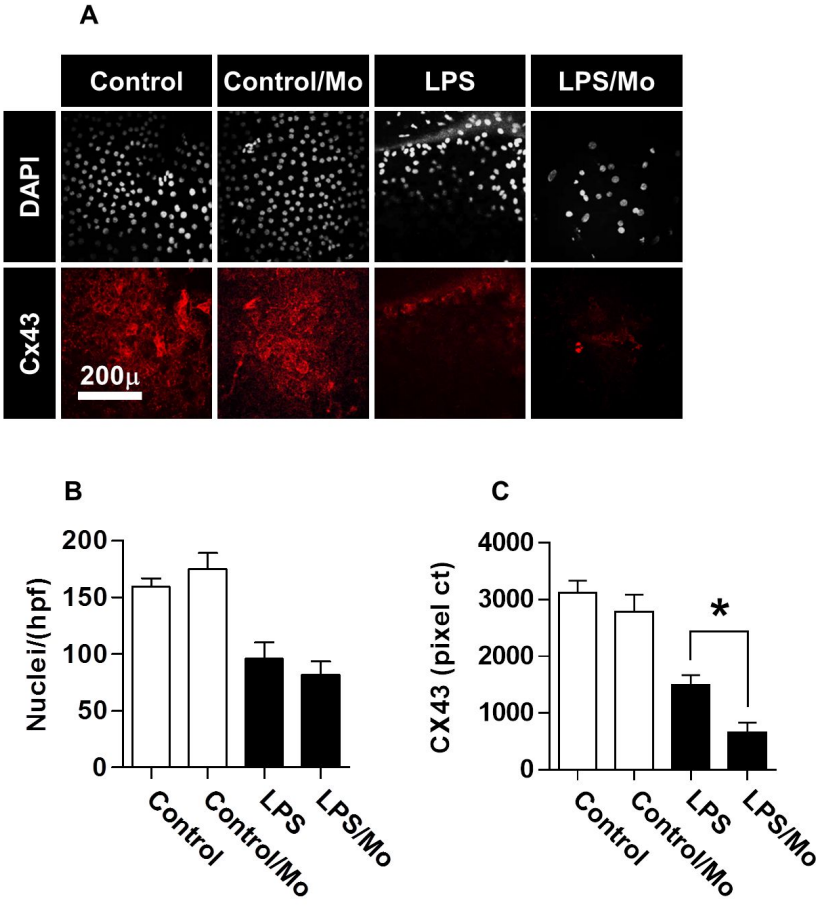
A
Control
Control/Mo
LPS
LPS/Mo
DAPI
Cx43
200µ
B
Nuclei/(hpf)
200
150
100
50
0
Control
Control/Mo
LPS
LPS/Mo
C
CX43 (pixel ct)
4000
3000
2000
1000
0
*
Control
Control/Mo
LPS
LPS/Mo

Figure 4

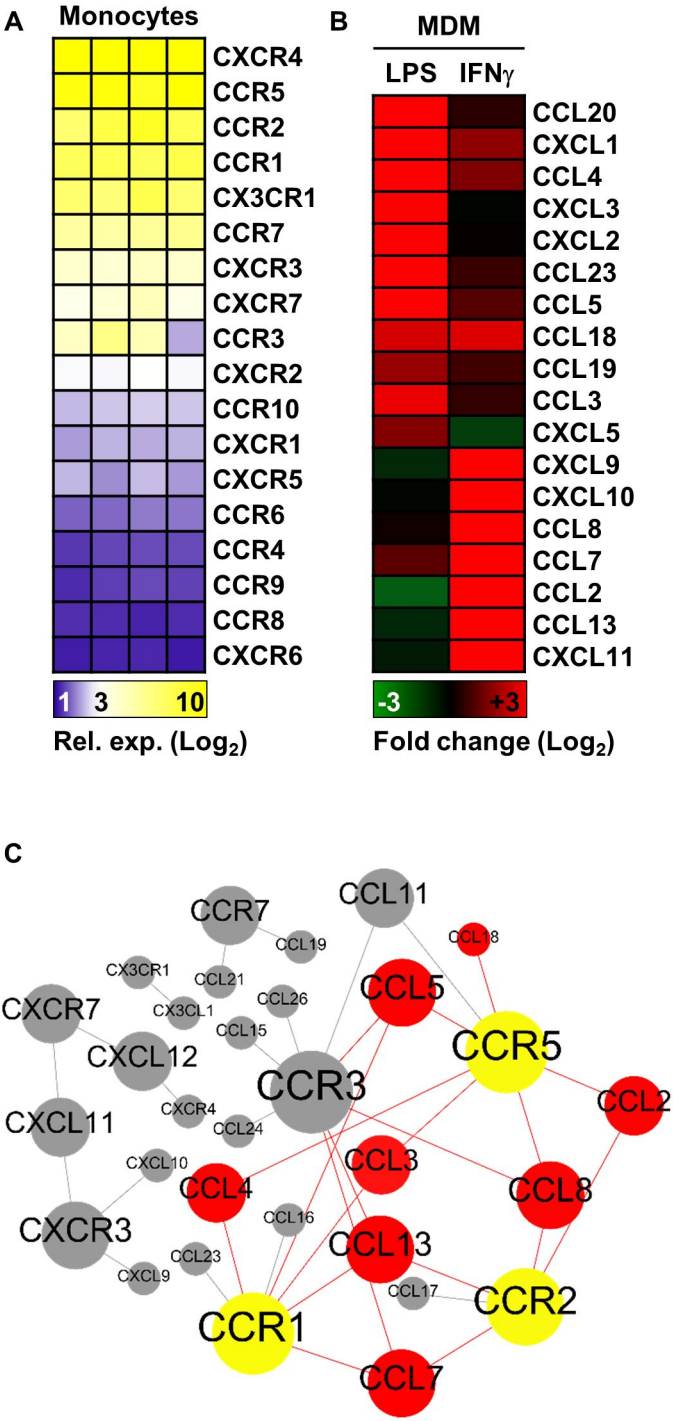
A
Monocytes
CXCR4
CCR5
CCR2
CCR1
CX3CR1
CCR7
CXCR3
CXCR7
CCR3
CXCR2
CCR10
CXCR1
CXCR5
CCR6
CCR4
CCR9
CCR8
CXCR6
1 3 10
Rel. exp. (Log2)
B
MDM
LPS IFNγ
CCL20
CXCL1
CCL4
CXCL3
CXCL2
CCL23
CCL5
CCL18
CCL19
CCL3
CXCL5
CXCL9
CXCL10
CCL8
CCL7
CCL2
CCL13
CXCL11
-3 +3
Fold change (Log2)
C
CCR7
CCL11
CCL19
CCL18
CX3CR1
CCL21
CCL5
CXCR7
CCL26
CX3CL1
CCL15
CCR5
CXCL12
CCR3
CCL2
CXCL11
CXCR4
CCL24
CXCL10
CCL3
CCL4
CCL8
CXCR3
CCL16
CCL13
CCL23
CXCL9
CCL17
CCR2
CCR1
CCL7

Figure 5

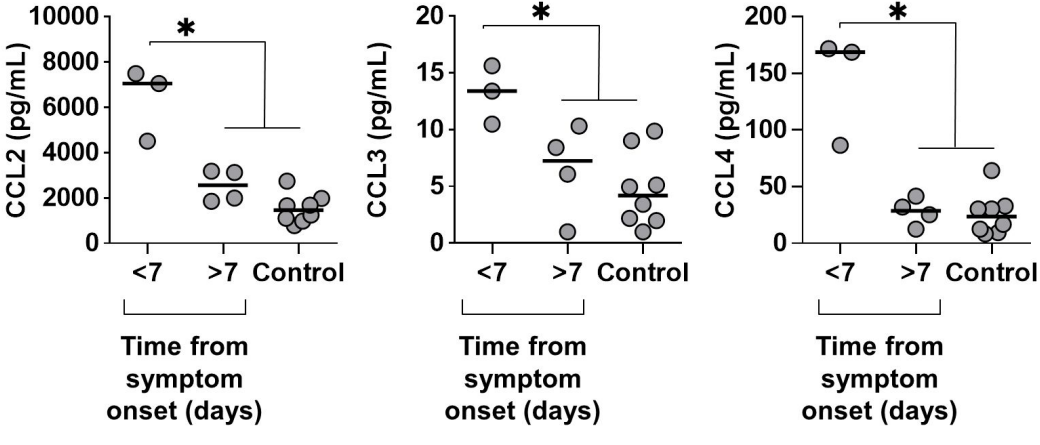
CCL2 (pg/mL)
10000
8000
6000
4000
2000
0
*
<7
>7
Control
Time from symptom onset (days)
CCL3 (pg/mL)
20
15
10
5
0
*
<7
>7
Control
Time from symptom onset (days)
CCL4 (pg/mL)
200
150
100
50
0
*
<7
>7
Control
Time from symptom onset (days)

Figure 6

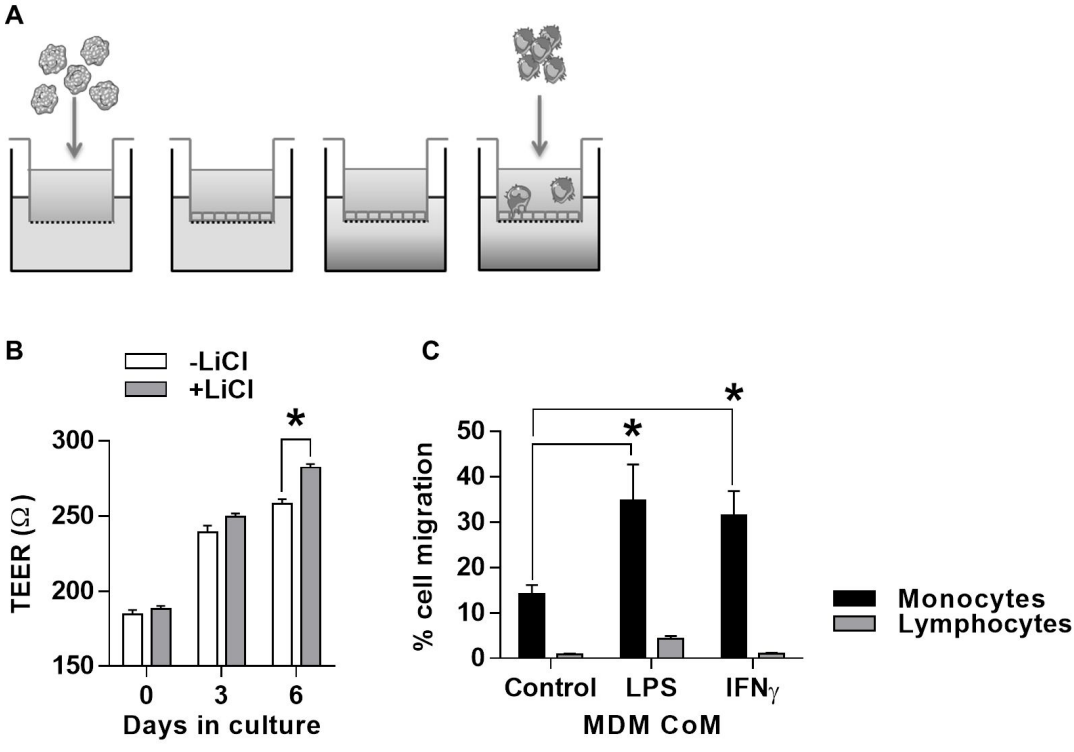
A
B
-LiCl
+LiCl
*
300
250
200
150
TEER (Ω)
0
3
6
Days in culture
C
*
*
50
40
30
20
10
0
% cell migration
Control
LPS
IFNγ
MDM CoM
Monocytes
Lymphocytes

Figure 7

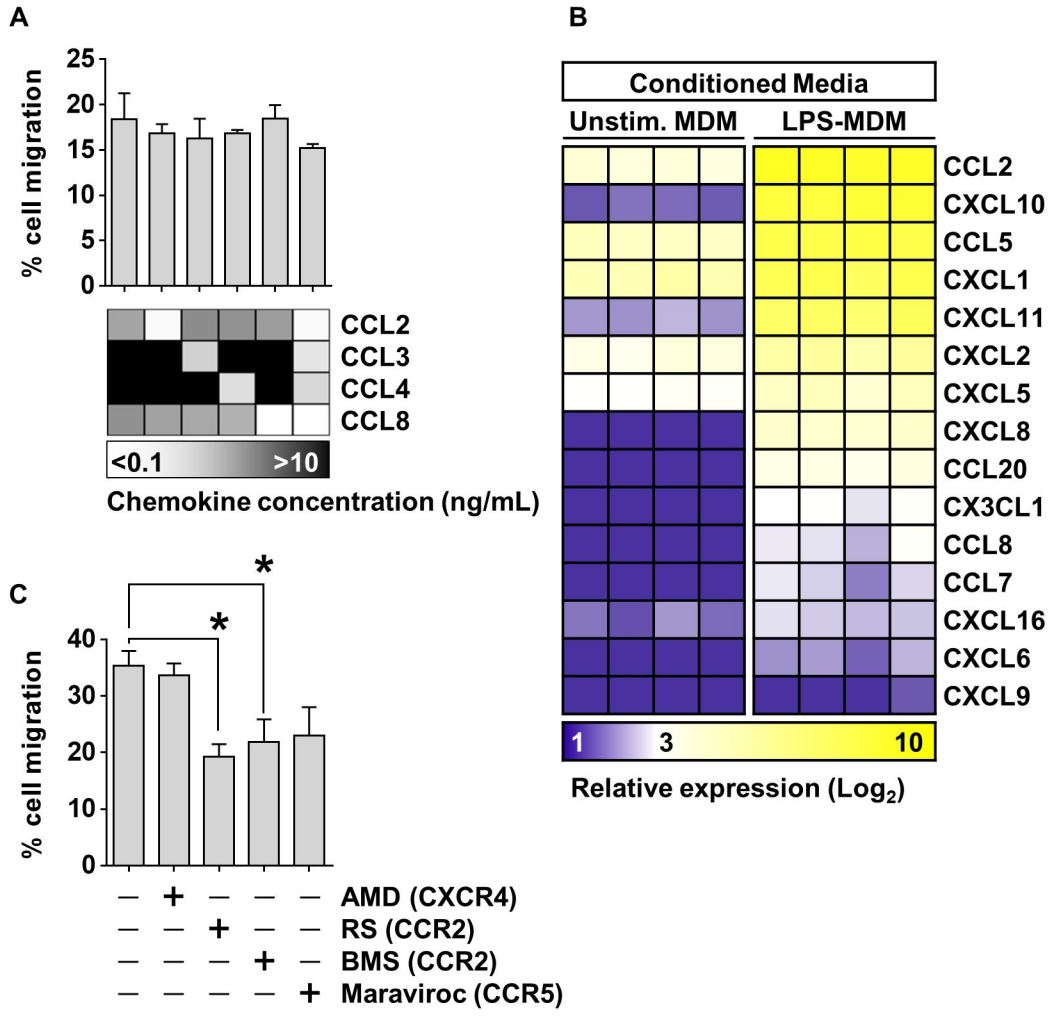
A
% cell migration
25
20
15
10
5
0
CCL2
CCL3
CCL4
CCL8
<0.1
>10
Chemokine concentration (ng/mL)
B
Conditioned Media
Unstim. MDM
LPS-MDM
CCL2
CXCL10
CCL5
CXCL1
CXCL11
CXCL2
CXCL5
CXCL8
CCL20
CX3CL1
CCL8
CCL7
CXCL16
CXCL6
CXCL9
1
3
10
Relative expression (Log2)
C
% cell migration
40
30
20
10
0
*
*
– + – – – AMD (CXCR4)
– – + – – RS (CCR2)
– – – + – BMS (CCR2)
– – – – + Maraviroc (CCR5)